Defect induced ferromagnetism in MgO nanoparticles studied by optical and positron annihilation spectroscopy

ARTICLE *in* CHEMICAL PHYSICS LETTERS · AUGUST 2009

Impact Factor: 1.9 · DOI: 10.1016/j.cplett.2009.07.037

3 AUTHORS:

Nitesh Kumar
Jawaharlal Nehru Centre for Advanced Scie…
42 PUBLICATIONS **297** CITATIONS
SEE PROFILE

Dirtha Sanyal
Variable Energy Cyclotron Centre
80 PUBLICATIONS **820** CITATIONS
SEE PROFILE

Sundaresan Athinarayanan
Jawaharlal Nehru Centre for Advanced Scie…
222 PUBLICATIONS **3,543** CITATIONS
SEE PROFILE

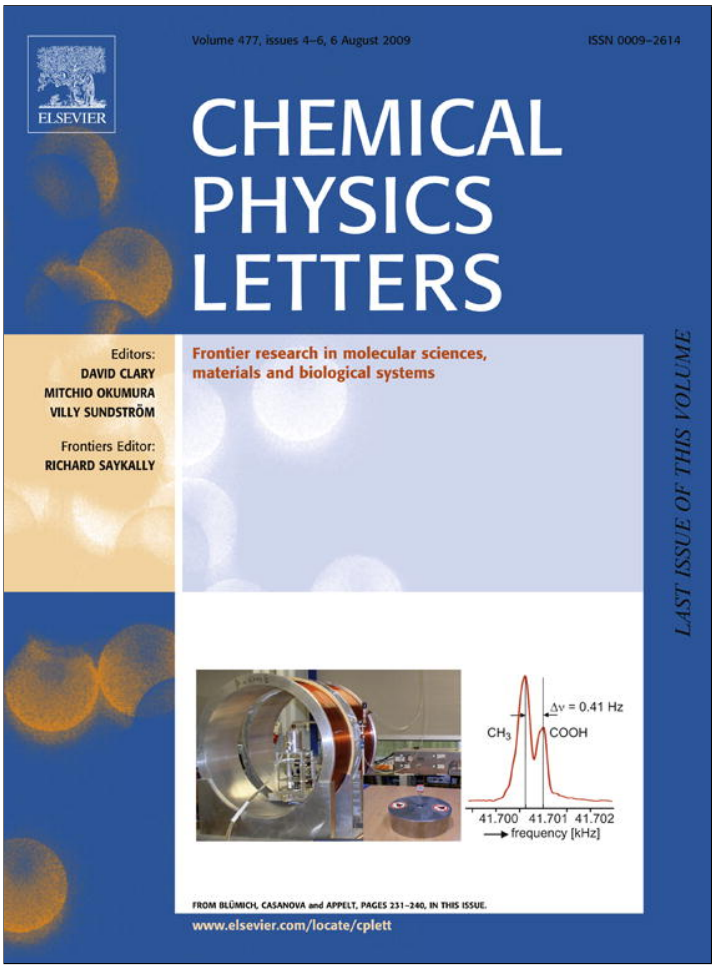

Chemical Physics Letters 477 (2009) 360–364

Contents lists available at ScienceDirect

Chemical Physics Letters

journal homepage: www.elsevier.com/locate/cplett

Defect induced ferromagnetism in MgO nanoparticles studied by optical and positron annihilation spectroscopy

Nitesh Kumar [a], D. Sanyal [b], A. Sundaresan [a,*]

[a] Chemistry and Physics of Materials Unit and Department of Science and Technology Unit on Nanoscience, Jawaharlal Nehru Centre for Advanced Scientific Research, Jakkur P.O., Bangalore 560 064, India
[b] Variable Energy Cyclotron Centre, 1/AF Bidhannagar, Kolkata 700 064, India

ARTICLE INFO

Article history:
Received 22 June 2009
In final form 9 July 2009
Available online 12 July 2009

ABSTRACT

Positron annihilation spectroscopy has been used to explore the nature of defects and to estimate the defect concentrations in ferromagnetic MgO nanoparticles. Our experimental results show that Mg vacancies or Mg vacancy concentration are present approximately at the concentration of 3.4×10^{16} cm^{-3} in the nano-crystalline MgO which is twice the value that obtained for bulk sample. This is in correlation with the decrease of the intensity of blue luminescence and the saturation magnetic moment with increasing particle size. These results clearly demonstrate that the origin of magnetic moment and thus the ferromagnetism in MgO nanoparticles is due to Mg related vacancies at the surface of the particles.

Recently, there has been a lot of interest in the study of magnetism in nanoparticles of the otherwise nonmagnetic inorganic materials because they exhibit ferromagnetism at room temperature [1–6]. The origin of magnetic moment in the nanoparticles of nonmagnetic materials was suggested to be due to cation or anion defects present at the surface of the particles. Thus, the ferromagnetism is confined to the surface of the nanoparticles while the core remains diamagnetic. The nature of defect responsible for magnetism seems to depend on specific material. For example, in oxide nanoparticles such as CeO_2 and TiO_2, oxygen vacancies induce magnetic moments on the Ce and Ti ions, respectively. In fact, presence of Ce^{4+}/Ce^{3+} and Ti^{4+}/Ti^{3+} mixed valence in nanoparticles of CeO_2 and TiO_2 have been evidenced from photoelectron spectroscopy [7,8]. Interestingly, the surface ferromagnetism was exploited to render the classic ferroelectric $BaTiO_3$ as multiferroic. First principles density functional calculations and positron annihilation experiments have shown the presence of oxygen vacancies in the nano-crystalline $BaTiO_3$ [6]. On the other hand, neutral cation vacancies have been suggested to be responsible for ferromagnetism in HfO_2 and CaO [9–11].

Following the suggestion that ferromagnetism is a universal feature of nanoparticles of the otherwise nonmagnetic materials [1], it has been shown experimentally through magnetization measurements that MgO nanoparticles also exhibit room temperature ferromagnetism [12]. Long ago, it was reported that neutral Mg vacancies induce large magnetic moment on neighboring oxygen ions [13]. Very recently, first-principles study on MgO has shown the appearance of collective ferromagnetism above a critical concentration (6.25%) of neutral Mg vacancies [14]. In this Letter, we report the experimental results of positron annihilation spectroscopy [15,16] to identify the nature of defects and also to estimate the defect concentration in nanoparticles as well as in bulk of MgO. We have also examined photoluminescence properties to correlate the defects and magnetism. Our results indeed show that Mg vacancy related defects are present in nanoparticles approximately at the concentration of $\sim 3.4 \times 10^{16}$ cm^{-3} which is two times higher than that of the bulk MgO. Further, the intensity of the luminescence band centered in the blue region associated with surface defects and the saturation magnetization decrease with increase of particles size demonstrate that the ferromagnetism in MgO nanoparticles originates from Mg related vacancies at the surface of the nanoparticles.

MgO nanoparticles were synthesized using high purity (99.99%) magnesium acetate tetrahydrate $(CH_3COO)_2Mg{\cdot}4H_2O$, polyvinyl pyrrolidone (PVP) and ethylene glycol (EG, 99.5%) as reported earlier [17]. 0.05 mol of magnesium acetate tetrahydrate and 0.3 mmol of PVP as capping agent were dissolved in EG in a round bottom flask. The solution was refluxed at 200 °C with constant stirring for 2 h to get a white flocculate. The reaction mixture was allowed to cool down to room temperature. The flocculate was collected by centrifuging the reaction mixture at 6000 rpm followed by washing with distilled water and then ethanol to remove remaining PVP and EG. Final drying of the flocculate was done at 80 °C in an oven to get magnesium oxide precursor. Precursor was calcined at 650, 750 and 850 °C for 2 h in oxygen atmosphere to form magnesium oxide nanoparticles of different sizes. Bulk

* Corresponding author. Fax: +91 8022082766.
E-mail addresses: dirtha@veccal.ernet.in (D. Sanyal), sundaresan@jncasr.ac.in (A. Sundaresan).

0009-2614/$ - see front matter © 2009 Elsevier B.V. All rights reserved.
doi:10.1016/j.cplett.2009.07.037

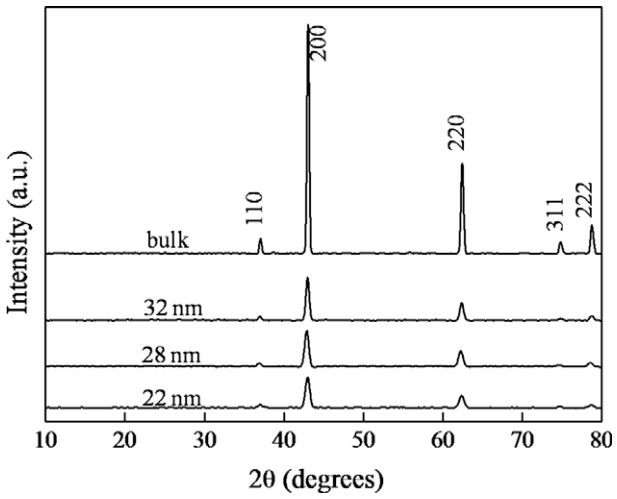

Fig. 1. XRD pattern of nanoparticles and bulk MgO.

magnesium oxide was prepared by palletizing the nanoparticles followed by sintering at 1450 °C in air.

X-ray diffraction (XRD) patterns were recorded with a Rigaku-99 diffractometer using Cu Kα radiation (λ = 1.5406 Å). Photoluminescence spectra were recorded in PERKIN–ELMER LS 55 Luminescence Spectrometer. Particle size and morphology were analyzed by Field Emission Scanning Electron Microscopy (FESEM) using NOVA NANOSEM 600 (FEI, The Netherlands). Magnetic measurements were carried out with vibrating sample magnetometer in Physical Properties Measurement System (PPMS, Quantum Design, USA).

For positron annihilation studies, a 10 μCi ^{22}NaCl source of positrons (enclosed between 2 μm thin nickel foils) was sandwiched [18–20] between two identical and plane faced pallets. The positron annihilation lifetime were measured with a fast-slow coincidence assembly. Detectors were 25-mm-diam × 25-mm-long cylindrical BaF_2 scintillators optically coupled to Philips XP2020Q photomultipliers tubes. The resolving time (full width at half maximum, FWHM) measured with a ^{60}Co source and with the windows of the slow channels of the fast–slow coincidence assembly set to select pulses corresponding to 300–550 keV in one channel and 700–1320 keV in the other, was 250 ps. For each positron annihilation lifetime spectrum about 10^6 coincidence counts were recorded. For each sample at least five to six positron annihilation lifetime spectra of about 10^6 coincidence counts were recorded to ensure the repeatability of the measurements. Measured positron annihilation lifetime was analyzed by computer programme PATFIT-88 [21] with necessary source corrections (446 ps of 4% intensity) to evaluate the possible lifetime component τ_i, and their corresponding intensities I_i. For the coincidence Doppler broadening of annihilation γ-radiation (CDBAR) measurement [22], two identical HPGe detectors (Efficiency: 12%; Type: PGC1216sp of DSG, Germany) of energy resolution 1.1 keV at 514 keV of ^{85}Sr was used as two 511 keV γ-ray detectors. The CDBAR spectrum was recorded in a dual ADC based – multiparameter data acquisition system (MPA-3 of FAST ComTec, Germany). The peak to background ratio of this CDBAR measurement system, with $\pm\Delta E$ selection, was $\sim 10^5$:1 [19,23,24]. CDBAR spectra were also analyzed by constructing the ratio curve.

XRD patterns of MgO particles annealed at different temperatures, as shown in Fig. 1, confirm that the sample is single phase with cubic structure. Scherrer formula was used to calculate particle size from peak broadening which comes about 22 nm for the sample annealed at 650 °C. The average particle size increases to 28, 32 nm for the sample annealed at 850 and 950 °C, respectively. The sample sintered at 1450 °C shows sharp lines in XRD pattern which is typical of bulk crystalline sample. These results are in agreement with FESEM images as shown in Fig. 2.

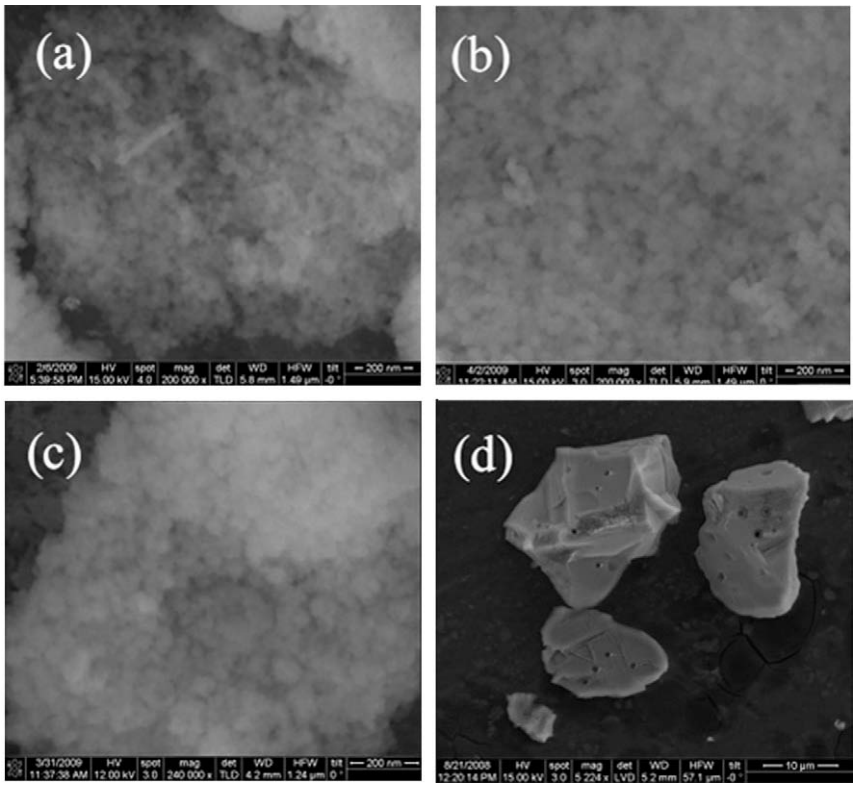

Fig. 2. FESEM images of nanoparticles: (a) 22 nm, (b) 28 nm, (c) 32 nm and (d) bulk MgO.

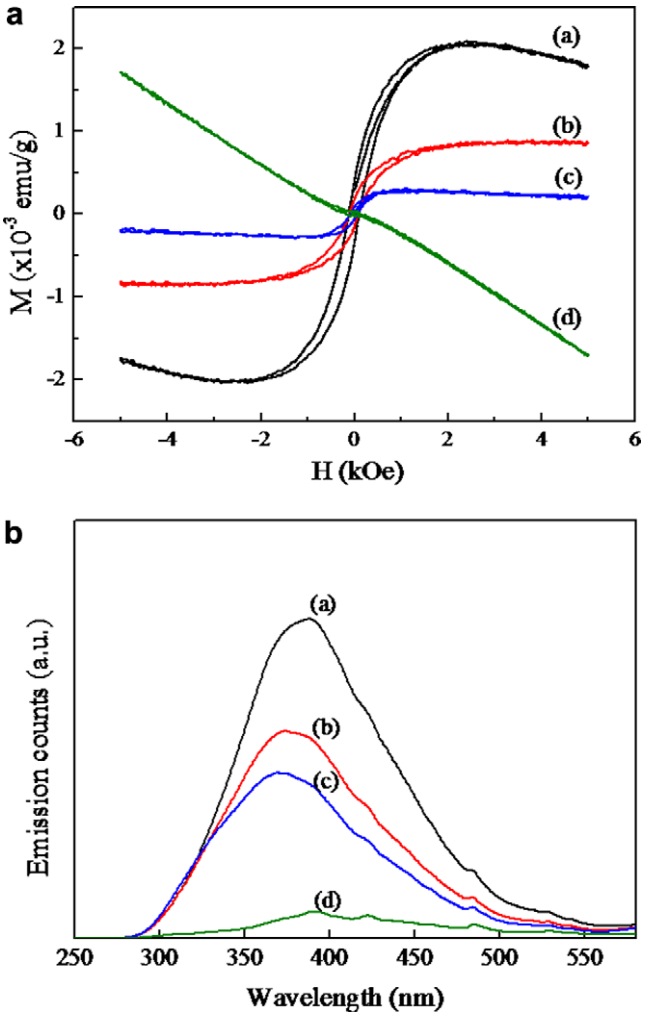

Fig. 3. (a) Room temperature magnetic hysteresis of nanoparticles: (a) 22 nm, (b) 28 nm, (c) 32 nm and (d) bulk MgO. (b) Photoluminescence spectra of (a) 22 nm, (b) 28 nm, (c) 32 nm and (d) bulk MgO.

Table 1
Positron lifetimes and corresponding intensities of 22 nm particles and bulk MgO.

Sample MgO	τ_1 (ps)	I_1 (%)	τ_2 (ps)	I_2 (%)	τ_3 (ps)	I_3 (%)	V_{Mg}
Bulk	161 ± 4	70 ± 1	385 ± 10	25 ± 1	1610 ± 50	5 ± 0.2	1.6×10^{16}
22 nm	168 ± 4	38 ± 1	400 ± 10	57 ± 1	1730 ± 50	5 ± 0.2	3.4×10^{16}

The results of magnetization measurements performed at 300 K on the three nanoparticles and bulk MgO are shown in Fig. 3a. All the nanoparticles show ferromagnetic hysteresis at room temperature. The saturation magnetization (0.00204 emu/g) is higher for the sample with smaller (22 nm) particles size. As the average particle size increases, the value of saturation magnetization decreases which is consistent with the earlier suggestion that magnetism comes from surface defects which decreases with increase of particles size due to decrease in surface to volume ratio [1]. The bulk sample which was heated at 1450 °C shows diamagnetic behavior as expected.

Optical properties of nanomaterials provide important information about the surface states. It is known that nanocrystals of MgO show a broad photoluminescence (PL) spectrum in the blue region due to low coordinated surface ions or defects [25–28]. It should be noted that bulk MgO does not show such luminescence spectrum consistent with relatively low concentration of surface defects. Fig. 3b shows PL spectra of the three nanoparticles and the bulk sample excited at the wavelength 225 nm. It can be seen that there is a broad peak centered around 370 nm whose intensity decreases with increase of particle size. Such a broad PL peak has already been reported in the literature and has been attributed to defects. In the present work, the observation that the peak intensity decreases with increase of particle size suggests that the concentration of surface defect decreases with increasing particle size.

In order to find the nature of defect and estimate its concentration, positron annihilation spectroscopy has been used. Table 1 shows the value of positron lifetimes, their corresponding intensities and finally the defect concentrations of 22 nm particles and bulk sample. The free fitting of all the positron lifetime spectra for both the samples (22 nm particles and bulk) are found to be best fitted (variance of fit is less than one per channel) with three lifetime components (Fig. 4) yielding a very long lifetime component (τ_3) with intensity (I_3) of 5 ± 0.2%. This component is due to the formation of *ortho*positronium and its subsequent decay as *para*positronium by pick-off annihilation processes. Positronium formation is always favourable in polycrystalline samples due to the presence of microvoids. The short lifetime component (τ_1) 161 ± 4 and 168 ± 4 ps for bulk and the 22 nm MgO sample, respectively, is generally attributed to the free annihilation of positrons. Theoretically calculated free positron lifetime in bulk MgO is 166 ps [29,30] which is in agreement with the presently observed values. The most important lifetime component is the intermediate one, τ_2, which arises from the annihilation of positrons at defect sites. In the present case τ_2 is found to be ~385 and 400 ps for the bulk and nano-crystalline MgO, respectively, which is coming from the annihilation of positron in the Mg vacancy type defect or Mg vacancy clusters. One can have an idea about the defect concentration from I_2, the intensity of the intermediate lifetime component. It is obvious from Table 1, that I_2 which is a measure of defect concentration is higher in nanoparticles (57%) than that in the bulk sample (25%). As the grain size decreases more positrons diffuse towards the grain surfaces and trapped in the defect sites present on the surface. Assuming an approximate specific trapping coefficient of $\mu_v \sim 3 \times 10^{15}\ s^{-1}$ at 300 K, similar to the Ga vacancy in GaN [31], the Mg vacancy in MgO has been calculated by the relation $[V_{Mg}] = N_{at}\mu_v^{-1}\tau_B^{-1}(\tau_{ave} - \tau_B)/(\tau_2 - \tau_{ave})$, where τ_B = bulk positron lifetime, τ_{ave} = average positron lifetime, τ_2 = positron

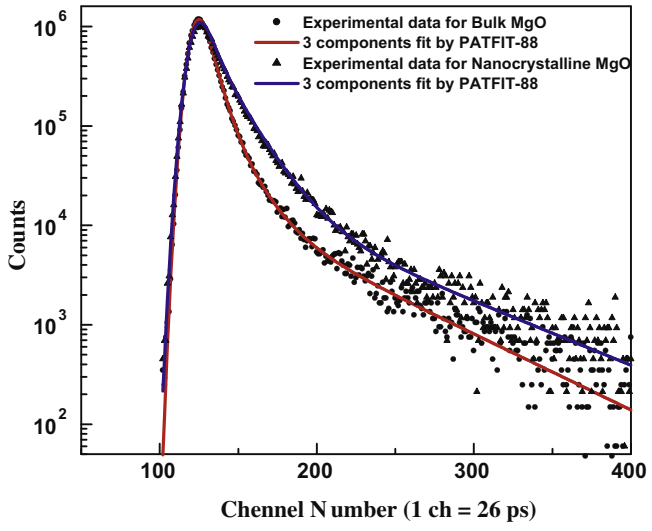

Fig. 4. The experimental positron lifetime spectrum, $N(t)$ vs. t, and the three lifetime components fitting curve by PATFIT-88 computer code for both 22 nm and bulk MgO.

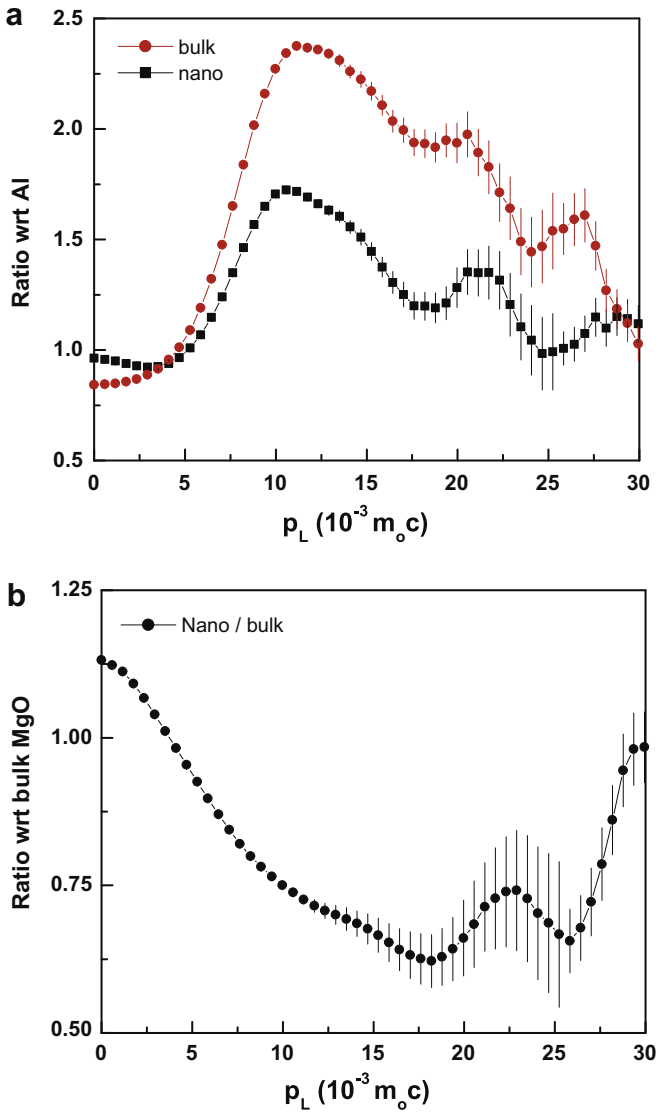

Fig. 5. (a) Area normalized ratio curves of 22 nm and bulk MgO CDBAR spectra with respect to defects free 99.9999% purity Al CDBAR spectrum. (b) Area normalized ratio curve of 22 nm MgO CDBAR spectrum with respect to bulk MgO CDBAR spectrum.

lifetime at defect site, N_{at} is the atomic density, in case of MgO it is $\sim 5 \times 10^{22}$ cm^{-3}. The Mg vacancy type defect in bulk MgO and nano-crystalline MgO comes out to be $(V_{Mg})_{Bulk} \sim 1.6 \times 10^{16}$ cm^{-3}; $(V_{Mg})_{Nano} \sim 3.4 \times 10^{16}$ cm^{-3}, respectively. Therefore, the suppression of magnetization with increase of particle size is in agreement with the decrease of defect concentration, since $(V_{Mg})_{Nano}/(V_{Mg})_{Bulk} \sim 2$.

Fig. 5a shows the area normalized ratio curve [32–35] of bulk and nano-crystalline MgO CDBAR spectra with respect to CDBAR spectrum of defects free 99.9999% purity Al sample. Both the ratio curves (Fig. 5a) show a major peak at $\sim 11 \times 10^{-3}$ m_oc, which is extended up to 30×10^{-3} m_oc. In general, the peak at momentum value $\sim 11 \times 10^{-3}$ m_oc in the ratio curve with respect to Al is mainly coming from the annihilation of positrons with the 2p electrons of oxygen [33] and some contributions coming from the annihilations of core electrons of Mg while the higher momentum region solely represents the annihilation of positrons with the core electrons of Mg. The most significant part of the Fig. 5a is that throughout the momentum range (5×10^{-3}–30×10^{-3} m_oc) the ratio curve for the nano-crystalline MgO is significantly less than that for bulk MgO. This picture is much clear in Fig. 5b where a ratio curve has been constructed between the CDBAR spectrum of nano-crystalline MgO with respect to the CDBAR spectrum of bulk MgO. Fig. 5b shows a prominent dip in the momentum value 17×10^{-3} m_oc, which indicates less annihilation of positrons with the core electrons of Mg in nano-crystalline MgO with respect to the bulk MgO. This indicates the presence of a significant amount of Mg vacancy in nano-crystalline MgO. Our results are consistent with the theoretical calculations on MgO which showed that neutral Mg vacancies induce large magnetic moment on neighboring oxygen ions similar to that reported for CaO [14]. They have also suggested that above a critical concentration of Mg vacancies (6.25%) these magnetic moments results in collective ferromagnetism.

In conclusion, we have studied the nature and concentration of defects using photoluminescence and positron annihilation spectroscopy in ferromagnetic MgO nanoparticles and compared with that of the bulk MgO. The intensity of photoluminescence which is a measure of defect concentration correlates with the decrease of saturation magnetization. Positron annihilation spectroscopy revealed the presence of Mg vacancies whose concentration decreases with increasing particle size which supports that Mg vacancies or Mg vacancy clusters are responsible for ferromagnetism in nanoparticles of MgO.

Acknowledgement

One of the authors (A.S.) is thankful to C.N.R. Rao for helpful discussions.

References

[1] A. Sundaresan, R. Bhargavi, N. Rangarajan, U. Siddesh, C.N.R. Rao, Phys. Rev. B 74 (2006) 16106.
[2] C. Madhu, A. Sundaresan, C.N.R. Rao, Phys. Rev. B 77 (2008) 201306.
[3] Shipra, A. Gomathi, A. Sundaresan, C.N.R. Rao, Solid State Commun. 142 (2007) 685.
[4] A. Sundaresan, C.N.R. Rao, Nanotoday 4 (2009) 96.
[5] A. Sundaresan, C.N.R. Rao, Solid State Commun. 149 (2009) 1197.
[6] R.V.K. Mangalam, N. Ray, U. Waghmare, A. Sundaresan, C.N.R. Rao, Solid State Commun. 149 (2009) 1.
[7] M. Li, S. Ge, W. Qiao, L. Zhang, Y. Zuo, S. Yan, Appl. Phys. Lett. 94 (2009) 152511.
[8] Q. Zhao, P. Wu, B.-L. Li, Z.-M. Lu, E.Y. Jiang, Chin. Phys. Lett. 25 (2008) 1811.
[9] A.D. Pemmaraju, S. Sanvito, Phys. Rev. Lett. 94 (2005) 217205.
[10] I.S. Elfimov, S. Yunoki, G.A. Sawatzky, Phys. Rev. Lett. 89 (2002) 216403.
[11] J. Osorio-Guillén, S. Lany, S.V. Barabash, A. Zunger, Phys. Rev. Lett. 96 (2006) 107203.
[12] J. Hu, Z. Zhang, M. Zhao, H. Qin, M. Jiang, Appl. Phys. Lett. 93 (2008) 192503.
[13] A.M. Stoneham, A.P. Pathak, R.H. Bartram, J. Phys. C: Solid State Phys. 9 (1976) 73.
[14] F. Gao et al., Solid State Commun. 149 (2009) 855.
[15] P. Hautojarvi, C. Corbel, in: A. Dupasquier, A.P. Mills Jr. (Eds.), Positron Spectroscopy of Solids, IOS Press, Ohmsha, Amsterdam, 1995.
[16] R. Krause-Rehberg, H.S. Leipner, Positron Annihilation in Semiconductors, Springer-Verlag, Berlin, 1999.
[17] A. Subramania, G. Vijaya Kumar, A.R.S. Priya, T. Vasudevan, Nanotechnology 18 (2007) 225601.
[18] D. Sanyal, D. Banerjee, U. De, Phys. Rev. B 58 (1998) 15226.
[19] D. Sanyal, T.K. Roy, M. Chakrabarti, S. Dechoudhury, D. Bhowmick, A. Chakrabarti, J. Phys. C 20 (2008) 045217.
[20] R.V.K. Mangalam, M. Chakrabrati, D. Sanyal, A. Chakrabarti, A. Sundaresan, Communicated, 2009.
[21] P. Kirkegaard, N.J. Pedersen, M. Eldroup, Report of Riso National Lab (Riso-M-2740), 1989.
[22] K.G. Lynn, A.N. Goland, Solid State Commun. 18 (1976) 1549.
[23] D. Sanyal, M. Chakrabarti, T.K. Roy, A. Chakrabarti, Phys. Lett. A 371 (2007) 482.
[24] S. Dutta, M. Chakrabarti, S. Chattopadhyay, D. Jana, D. Sanyal, A. Sarkar, J. Appl. Phys. 98 (2005) 053513.
[25] S. Stankic, M. Muller, O. Diwald, M. Sterrer, E. Knozinger, J. Bernardi, Angew. Chem., Int. Ed. 44 (2005) 4917.
[26] S.G. Maclean, W.W. Duley, J. Phys. Chem. Solid 45 (1984) 227.
[27] M. Anpo, Y. Yamada, Y. Kubokawa, S. Coluccia, A. Zecchina, M. Che, J. Chem. Soc., Faraday Trans. I 84 (3) (1998) 751.
[28] C. Chizallet, G. Costentin, H.L. Pernot, J.M. Krafft, M. Che, F. Delbecq, P. Sautet, J. Phys. Chem. C 112 (2008) 16629.
[29] M.J. Puska, S. Mäkinen, M. Manninen, R.M. Nieminen, Phys. Rev. B 39 (1989) 7666.
[30] R. Pareja, Positron Annihilation, World Scientific, Singapore, 1985. p. 708.

[31] K. Saarinen, Phys. Rev. B 64 (2001) 233201.
[32] P. Asoka-Kumar, M. Alatalo, V.J. Ghosh, A.C. Kruseman, B. Nielsen, K.G. Lynn, Phys. Rev. Lett. 77 (1996) 2097.
[33] R.S. Brusa, W. Deng, G.P. Karwasz, A. Zecca, Nucl. Instrum. Method B 194 (2002) 519.
[34] M. Chakrabarti, A. Sarkar, D. Sanyal, G.P. Karwasz, A. Zecca, Phys. Lett. A 321 (2004) 376.
[35] S. Dutta, S. Chattopadhyay, A. Sarkar, M. Chakrabarti, D. Sanyal, D. Jana, Prog. Mater. Sci. 54 (2009) 89.